

Topologically protected pure helicity cascade in non-Abelian quantum turbulence

Michikazu Kobayashi¹ and Masahito Ueda^{2,3}

¹*Department of Physics, Kyoto University, Oiwake-cho,
Kitashirakawa, Sakyo-ku, Kyoto 606-8502, Japan,*

²*Department of Physics, University of Tokyo, Hongo 7-3-1, Bunkyo-ku, Tokyo 113-0033, Japan,*

³*RIKEN Center for Emergent Matter Science (CEMS), Wako, Saitama 351-0198, Japan*

(Dated: August 29, 2018)

By numerically studying non-Abelian quantum turbulence, we find that the helicity cascade and the inverse energy cascade are topologically protected against reconnection of vortices and lead to the energy spectrum $E(k) \propto k^{-7/3}$ for a large-scale energy injection and $E(k) \propto k^{-5/3}$ for a small-scale energy injection with a large-scale web of non-Abelian vortices. Our prediction can be tested in the cyclic phase of a spin-2 spinor Bose-Einstein condensate.

Introduction.— Turbulence is a highly nonequilibrium and dynamically nonstationary phenomenon that appears in a variety of macroscopic systems [1]. Yet it exhibits stationary statistical laws, culminating in Kolmogorov's $-5/3$ law [2, 3] in an inertial range where the energy flows to smaller scales at a constant flux, which is known as the energy cascade.

Turbulence is characterized by the universality class, conservation laws, and cascades of physical quantities in the inertial range. In Kolmogorov's law, the kinetic energy is the conserved quantity. In two dimensions, there is another conserved quantity – the enstrophy which is defined as the square of the fluid vorticity. Two-dimensional steady turbulence therefore belongs to a different universality class supported by the enstrophy cascade, featuring the energy spectrum $E(k) \propto k^{-3}$ at small scales and Kolmogorov's $-5/3$ law at large scales [4]. In three dimensions, there is yet another conserved quantity – the helicity which is given as the inner product of the fluid velocity and vorticity [5, 6]. However, its contribution to turbulence is small [7, 8] because the direction of the helicity cascade is the same as that for the energy cascade in marked contrast to the energy and enstrophy cascades in two-dimensional turbulence, leaving the Kolmogorov's spectrum unchanged [9, 10].

Quantum turbulence exhibits a spatially and dynamically complex structure of quantized vortices [11]. Like classical turbulence, quantum turbulence also features Kolmogorov's $-5/3$ law associated with the energy cascade [12]. The helicity cascade has also been observed in large-scale quantum turbulence simulations [13], showing the helicity spectrum with the $-5/3$ power law. In this Letter, we propose non-Abelian quantum turbulence as a new theoretical paradigm of turbulence, and report the universality class characterized by the topologically protected pure helicity cascade. Non-Abelian vortices are defined as those having non-Abelian topological charges classified by the fundamental group [14]. The crucial distinction between Abelian and non-Abelian vortices manifests itself in the collision dynamics. The collision of two Abelian vortices mostly leads to reconnection [15] and causes a topological change in the geometric structure of vortices; vortices are broken up into smaller ones. Non-Abelian vortices, in contrast, do not reconnect due to the

topological constraint [16], and short vortices are nucleated that bridge colliding vortices, leading to a large-scale web of non-Abelian vortices. A unique universality class of turbulence is shown to emerge as a consequence of the pure helicity cascade and the inverse energy cascade in contrast to Abelian quantum turbulence characterized by energy and helicity cascades into the same direction, i.e., from larger to smaller scales.

As a simplest superfluid system that supports non-Abelian vortices, we consider the cyclic phase of a spin-2 spinor Bose-Einstein condensate (BEC) and its turbulent state with energy injection and dissipation. We find a unique power-law energy spectrum $E(k) \propto k^{-7/3}$ with a large-scale energy injection instead of Kolmogorov's law in Abelian quantum turbulence [12], and show that this power-law spectrum is directly connected to the pure helicity cascade without the energy cascade. The energy spectrum shows Kolmogorov's $-5/3$ power law again with a small-scale energy injection, supporting the inverse energy cascade from small to large scales. These findings unveil the universality class characterized by the $-7/3$ power law due to the topologically protected pure helicity cascade. We have also performed simulations in other BEC systems such as spin-1 spinor BECs and a two-component BEC with and without the quadratic Zeeman effect and found no evidence of this peculiar power law.

Model.— The Hamiltonian \mathcal{H} of the spin-2 BEC is given by [17]

$$\mathcal{H} = \int d^3x \left\{ \frac{\hbar^2}{2M} \sum_{m=-2}^2 |\nabla \psi_m|^2 + \frac{g_0}{2} (\rho - \bar{\rho})^2 + \frac{g_1}{2} \mathbf{S}^2 + \frac{g_2}{2} |A|^2 \right\}, \quad (1)$$

where $\psi = (\psi_2, \psi_1, \psi_0, \psi_{-1}, \psi_{-2})^T$ is the spinor order parameter in the irreducible representation (T denotes the transpose), M is the atomic mass, $\rho = \sum_{m=-2}^2 |\psi_m|^2$ is the total number density with $\bar{\rho}$ being its mean, and $\mathbf{S} = \sum_{m,n=-2}^2 \psi_m^* [\hat{\mathbf{S}}]_{m,n} \psi_n$ and $A = \sum_{m=-2}^2 \psi_m \psi_{-m}$ are the spin vector density and the spin-singlet pair amplitude, respectively with $\hat{\mathbf{S}}$ being the vector of spin-2 matrices. The ground state for the positive coupling constants

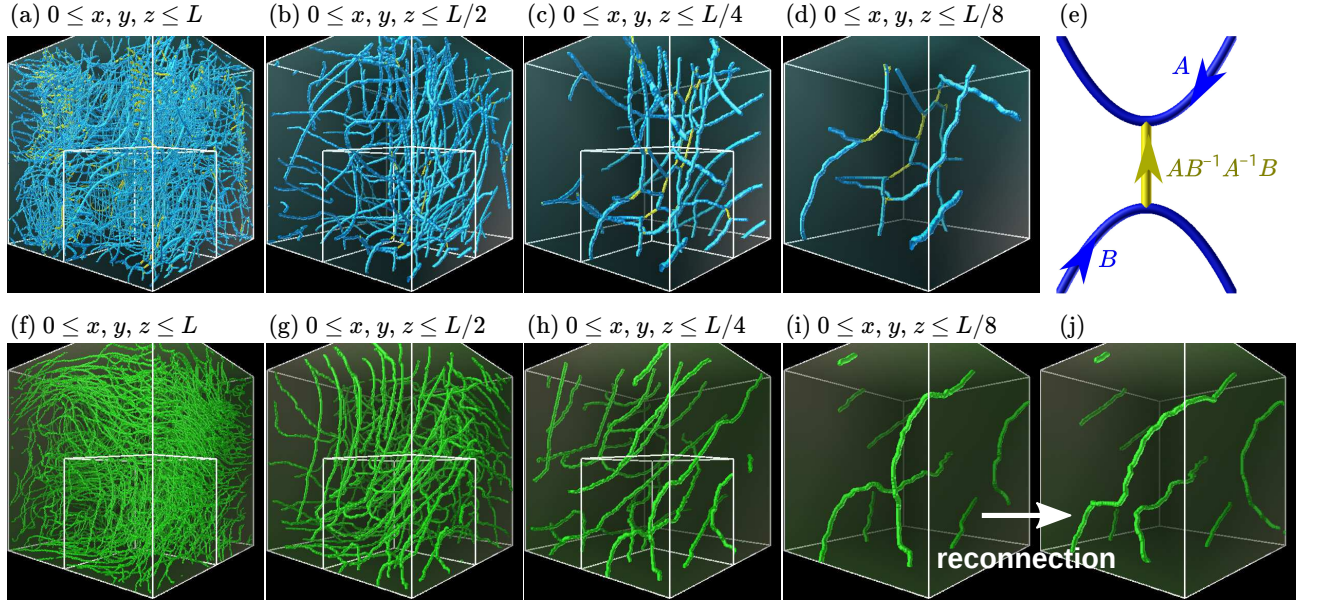


FIG. 1. Snapshots of quantum turbulence with the large-scale current $\mathbf{v}_{\text{ext}}^L$ for a non-Abelian spin-2 spinor BEC (upper panels) compared with those of an Abelian scalar BEC (lower panels). In upper panels, blue and yellow curves show vortices with circulations $\kappa_{\text{cyclic}} = h/(3M)$ and 0, respectively. In lower panels, green curves show vortices with circulation $\kappa_{\text{scalar}} = h/M$. The leftmost upper and lower panels show vortices in the entire region ($0 \leq x, y, z \leq L$) and each of the following pair show the enlarged views: $0 \leq x, y, z \leq L/2$ in (b) and (g), $0 \leq x, y, z \leq L/4$ in (c) and (h), and $0 \leq x, y, z \leq L/8$ in (d) and (i). In upper panels, blue-colored vortices are bridged by yellow-colored vortices, forming a large-scale web of non-Abelian vortices. A rung formation is clearly seen in (d) as a consequence of the non-commutative nature of the two colliding vortices as schematically illustrated in (e), where two non-Abelian vortices with the circulation κ_{cyclic} having topological charges A and B are bridged by a rung vortex whose topological charge is $AB^{-1}A^{-1}B$. Note that this charge would become trivial (i.e. equal to 1) for Abelian vortices for which A and B commute. In lower panels, green colored vortices are not connected unlike non-Abelian vortices because they can reconnect upon collision. In (i), two vortices reconnect and change their spatial configuration as shown in (j).

$g_{0,1,2} > 0$ belongs to the cyclic phase where both \mathbf{S} and \mathbf{A} vanish [18]. A representative state of the cyclic phase is given by $\psi_{\text{cyclic}} = \sqrt{\rho} e^{i\phi} e^{-i\mathbf{S} \cdot \mathbf{n}\theta} (i/2, 0, 1/\sqrt{2}, 0, i/2)^T$ [19], where $\phi \in [0, 2\pi/3)$ is the $U(1)$ phase, and \mathbf{n} and θ are the unit vector of the rotation axis and the rotation angle, respectively. Quantized vortices appear as topological excitations and play a major role in quantum turbulence. For the cyclic phase, vortices can have zero and two fractional circulations $0, h/(3M) \equiv \kappa_{\text{cyclic}}$, and $2\kappa_{\text{cyclic}}$, where the first two make major contributions to turbulence because the last one is energetically costly [20].

Simulation of turbulence.—

The dynamics of the system is governed by the non-linear Schrödinger equation: $i\hbar\partial_t\psi_m = \delta\mathcal{H}/\delta\psi_m^*$. To obtain a statistical steady state of turbulence, we need to introduce energy injection and dissipation. Dissipation is introduced through elimination of the Fourier components of ψ_m with high wavenumbers $k > k_c$ at each instant of time. Energy injection is introduced by an external current \mathbf{v}_{ext} through the non-uniform gauge: $\nabla \rightarrow \nabla - iM/(2\hbar)\mathbf{v}_{\text{ext}}$. We perform numerical simulations in the periodic box with 2048^3 grids. The space is discretized by the grids with the spacing $\Delta x = 0.25\xi$, where the healing length $\xi \equiv \hbar/\sqrt{2Mg_0\rho}$ has the same

order of magnitude as the size of a vortex core. The cutoff wavenumber k_c for the truncation of the wave function is set to be $k_c = 2\pi/\xi$. The coupling constants are chosen to be $g_{1,2} = 0.5g_0$ in the present simulations. The external current \mathbf{v}_{ext} is determined as the superposition of cosine waves with random phases: $(v_{\text{ext}})_{x,y,z} = \bar{v} \sum_{0 \leq |\mathbf{n}| \leq n_c} \cos(2\pi\mathbf{n} \cdot \mathbf{x}/L + \theta_{\mathbf{n},x,y,z})$, where $\mathbf{n} \in \mathbb{Z}^3$, the system size $L = 512\xi$, and $\theta_{\mathbf{n},i}$ is uniformly distributed over $[0, 2\pi)$ for each \mathbf{n} and $i = x, y, z$. We prepare two external currents; a large-scale current $\mathbf{v}_{\text{ext}}^L$ with $n_c = 2$ and $\bar{v} = 0.4\sqrt{g_0\rho/M}$, and a small-scale current $\mathbf{v}_{\text{ext}}^S$ with $n_c = 32$ and $\bar{v} = 0.1\sqrt{g_0\rho/M}$. We have used the pseudo-spectral method in space and the fourth-order Runge-Kutta method in time.

After a long-time evolution, the statistical steady state of quantum turbulence with a large number of vortices is achieved. Figures 1 (a)-(d) show snapshots of vortices with the large-scale current $\mathbf{v}_{\text{ext}}^L$. As a comparison, we also perform numerical simulations for a scalar BEC with every vortex having the unit circulation $\kappa_{\text{scalar}} = h/M$ under the same condition and obtain the corresponding statistical steady state as shown in Fig. 1 (f)-(i). We use $n_c = 2$ and $\bar{v} = 0.8\sqrt{g_0\rho/M}$, and obtain almost the same total vortex length as that for the cyclic state. We calculate the kinetic energy spectrum $E(k)$ per unit mass

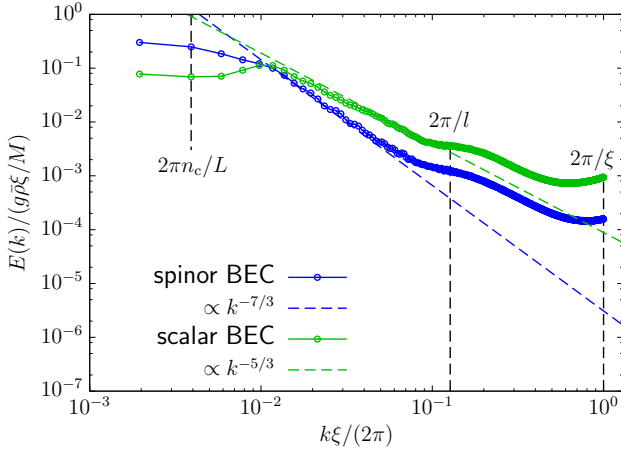


FIG. 2. Energy spectra $E(k)$ of the fluid velocity for turbulence of a spin-2 BEC (blue curve) and a scalar BEC (green curve) with the large-scale current $\mathbf{v}_{\text{ext}}^L$. The green dashed line shows Kolmogorov's law $\propto k^{-5/3}$ due to the energy cascade for $k < l^{-1}$. The blue dashed line shows the spectrum $E(k) \propto k^{-7/3}$ for the helicity cascade at $k < l^{-1}$ (see the main text). Here $l = \sqrt{1/\rho_{\text{vortex}}}$ is the mean inter-vortex spacing and takes $l \simeq 15.7\xi$ for the spinor BEC and $l \simeq 15.5\xi$ for the scalar BEC, and $\xi = \hbar/\sqrt{2Mg_0\rho}$ is the healing length. The ensemble average is taken over 200 steady states generated for different $\mathbf{v}_{\text{ext}}^L$.

defined as [21]

$$\int dk E(k) = \frac{1}{2} \int d^3x \rho \mathbf{v}^2 \equiv E_v, \quad (2)$$

where \mathbf{v} is the superfluid velocity defined as $\rho \mathbf{v} = \bar{\kappa} \sum_{m=-2}^2 \text{Im}[\psi_m^* \nabla \psi_m]$ with $\bar{\kappa} \equiv \hbar/M$ [17]. The energy spectrum $E(k)$ for the cyclic state of the spinor BEC is plotted as a blue curve in Fig. 2 which shows a power-law for $k < l^{-1}$, where $l = 1/\sqrt{\rho_{\text{vortex}}}$ is the mean intervortex spacing with the vortex length density ρ_{vortex} [22]. Compared with the energy spectra $E(k)$ for the scalar BEC (green curve) which shows Kolmogorov's law for $k < l^{-1}$ [23], $E(k)$ for the cyclic phase clearly deviates from Kolmogorov's law and its slope is steeper. This result suggests that the energy resides in large-scale web of non-Abelian vortices. Fitting the data in Fig. 2 with $E(k) \propto k^{-\eta}$ for $8\pi/L < k < 48\pi/L$, we find $\eta \simeq 2.28(5)$ which is consistent with $7/3$.

Helicity cascade and inverse energy cascade.— We argue that the physics behind the $-7/3$ power-law spectrum is the pure helicity cascade. In the inertial range far from the energy-injecting range and the energy-dissipative range, we suppose that the helicity H defined by $H \equiv (1/L^3) \int d^3x \mathbf{v} \cdot (\nabla \times \mathbf{v})$ is approximately conserved with neither energy injection nor dissipation, and cascades into the region at higher wavenumbers [13, 24]. Because helicity has the dimension $[LT^{-2}]$, the helicity flux ε_H per unit time in the wavenumber space has the dimension $[LT^{-3}]$. Provided that the energy spectrum has a scale invariant power-law structure and is determined

only from the helicity flux ε_H in the inertial range, we obtain the energy spectrum $E(k) \propto \varepsilon_H^{2/3} k^{-7/3}$. However, the $-7/3$ power-law spectrum is screened out by the standard Kolmogorov's power-law spectrum when the energy also cascades with the helicity, and can be seen only when the helicity solely cascades. The result of our numerical simulation in Fig. 2 suggests, therefore, the pure helicity cascade in non-Abelian quantum turbulence.

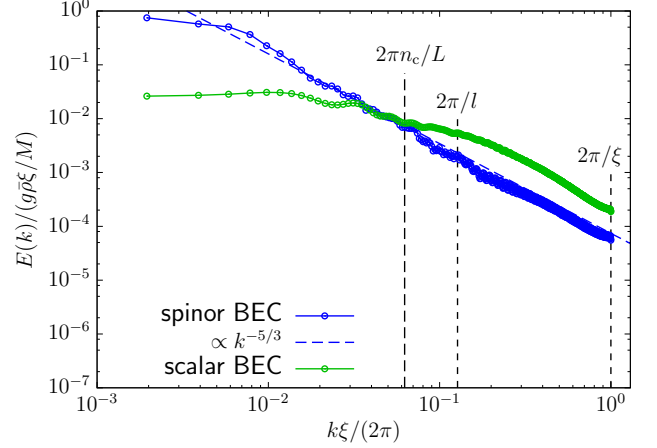


FIG. 3. Energy spectra $E(k)$ of the fluid velocity for turbulence of a spin-2 BEC (blue curve) and a scalar BEC (green curve) with the small-scale current $\mathbf{v}_{\text{ext}}^S$. The blue dashed line shows Kolmogorov's law $\propto k^{-5/3}$ due to the energy cascade for $k < l^{-1}$. The mean inter-vortex spacing takes $l \simeq 15.4\xi$ for the spinor BEC and $l \simeq 15.1\xi$ for the scalar BEC. The ensemble average is taken over 200 steady states generated for different $\mathbf{v}_{\text{ext}}^S$.

A question arises as to why the energy does not cascade. To answer this question, we perform another numerical calculation with the small-scale current $\mathbf{v}_{\text{ext}}^S$. Figure 3 shows the energy spectrum with $\mathbf{v}_{\text{ext}}^S$. The energy spectrum $E(k)$ for the cyclic state of the spinor BEC (blue curve) shows Kolmogorov's $-5/3$ power-law at low wavenumbers $k \lesssim 2\pi n_c/L$. For the scalar BEC with $n_c = 32$ and $\bar{v} = 0.2\sqrt{g_0\rho/M}$, $E(k)$ has no power-law structure (green curve). Kolmogorov's power spectrum for the cyclic state of the spinor BEC suggests the inverse energy cascade in the direction from small to large scales as seen in two-dimensional turbulence. We can explain the pure helicity cascade in Fig. 2 as opposite directions of the energy and helicity cascades. Figure 4 shows snapshots of vortices in quantum turbulence. Compared with the scalar BEC shown in panel (b), almost all vortices are connected through rung vortices making a large-scale web of non-Abelian vortices as shown in panel (a) for the cyclic state of the spinor BEC, suggesting that the inverse energy cascade generates a vortex network from smaller vortices.

Discussion and concluding remarks.— We have numerically studied the steady state of fully developed non-Abelian quantum turbulence. The obtained kinetic energy spectrum shows a unique $-7/3$ power law with the

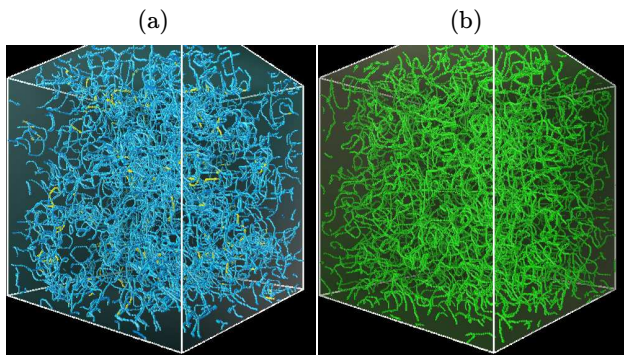


FIG. 4. Snapshots of quantum turbulence with the small-scale current $\mathbf{v}_{\text{ext}}^{\text{S}}$ for the cyclic state of the spinor BEC (panel (a)) and the scalar BEC (panel (b)). We use the same colors for vortices as those used in Fig. 1. In panel (a), rung vortices (yellow color) bridge almost all vortices (blue color) making a large-scale vortexweb, whereas in panel (b) vortices are separated with independent loops.

large-scale energy injection. This exponent is directly related to the pure helicity cascade without the energy cascade. To support the validity of the pure helicity cascade in non-Abelian quantum turbulence, we have also performed a turbulence simulation with the small-scale energy injection. The energy spectrum shows Kolmogorov's $-5/3$ power law, suggesting the inverse energy cascade which never occurs in standard three-dimensional turbulence including classical-fluid turbulence and Abelian quantum turbulence.

To discuss the pure helicity cascade and the inverse energy cascade, we must consider the helicity in quantum fluid. In a nonmagnetic phase such as the cyclic phase of the spinor BEC, the helicity density $\mathbf{v} \times (\nabla \times \mathbf{v})$ vanishes everywhere except for vortex cores at which it diverges [17]. Instead of the original definition, we can consider the center-line helicity [13, 24, 25] $H = \kappa_{\text{cyclic, scalar}}^2 (N_{\text{twist}} + T_{\text{torsion}})/L^3$, where $N_{\text{twist}} \in \mathbb{Z}$ is the total twist of the global phase and $T_{\text{torsion}} \in \mathbb{R}$ is the total torsion along vortex lines. Here N_{twist} represents the topological part of the helicity comprised of the links and writhes of vortices. When vortices are Abelian, reconnections can change the twist N_{twist} to the torsion T_{torsion} which is the non-topological part of the helicity such as Kelvin waves while approximately conserving the total helicity H [13, 15, 24–26]. For non-Abelian vortices, on the other hand, reconnections are topologically prohibited and the twist N_{twist} itself is conserved, leading to conserved knotted structures of vortices. Another feature of non-Abelian vortices is that two colliding vortices form a rung vortex that bridges them and almost

all vortices are connected, leading to a large-scale web of non-Abelian vortices as can be seen in Figs. 1 (a) and 4 (a). We expect that the helicity cascade is caused by formations of rung vortices as well as reconnections in Abelian turbulence [13], whereas the inverse energy cascade is strongly related to the above two important features of non-Abelian vortices, i.e., the conservation of the twist part N_{twist} of the helicity and the formation of the large-scale vortex network.

The pure helicity and the inverse energy cascade have been observed in the three-dimensional modified Navier-Stokes turbulence [27]. Our observation may help us understand more about the relationship between the helicity cascade and the topological structure of vortices, and the necessary conditions for the existence of the pure helicity cascade. Furthermore, there are other systems in which non-Abelian topological defects appear, such as crystals (dislocation and disclination) [28], liquid crystals (disclination) [29], and cosmology (cosmic strings) [30, 31], and our result may have implications for their non-equilibrium dynamics. One important application of our observation is a neutron star in which two neutrons form a Cooper pair showing superfluidity. The symmetry of the Cooper pair is predicted to be the triplet 3P_2 state [32] which has the same internal degrees of freedom as those of the spin-2 spinor BEC. If the stable ground state of the 3P_2 state in some neutron star is the cyclic state or other states that involve non-Abelian vortices, we can expect that the non-Abelian quantum turbulence undergoing the pure helicity cascade and the inverse energy cascade is realized in the neutron star and its signal may be observed as, for example, the energy release in macroscopic scales transported through the inverse energy cascade.

ACKNOWLEDGMENTS

We would like to thank Marc E. Brachet, Davide Proment, Naoki Yamamoto, Calro F. Barenghi, Ionut Danaila, and Shin-ichi Sasa for the helpful suggestions and comments. The work of MK is supported in part by Grant-in-Aid for Scientific Research No. 26870295 and by Grant-in-Aid for Scientific Research on Innovative Areas “Fluctuation & Structure” (No. 26103519) from the Ministry of Education, Culture, Sports, Science and Technology of Japan. MU acknowledges the support by KAKENHI Grant No. 26287088 from the Japan Society for the Promotion of Science and a Grant-in-Aid for Scientific Research on Innovative Areas “Topological Materials Science” (KAKENHI Grant No. 15H05855) and the Photon Frontier Network Program from MEXT.

[1] U. Frisch, “*Turbulence*” (Cambridge University Press, Cambridge, 1995).

[2] A. N. Kolmogorov, Proc. R. Soc., Sect. A **434**, 9 (1991); A. N. Kolmogorov, Proc. R. Soc., Sect. A **434**, 15 (1991).

- [3] G. K. Batchelor, “*The Theory of Homogeneous Turbulence*” (Cambridge University Press, Cambridge, 1953).
- [4] R. H. Kraichnan, Phys. Fluid, **10**, 1417 (1967).
- [5] W. Thomson, Trans. Roy. Soc. Edin. **25**, 217 (1868).
- [6] H. K. Moffatt, J. Fluid Mech. **35** 117 (1969); H. K. Moffatt and R. L. Ricca, Proc. R. Soc. Lond. A **439**, 411 (1992).
- [7] R. H. Kraichnan, J. Fluid Mech. **59**, 745 (1973).
- [8] V. Borue and S. A. Orszag, Phys. Rev. E **55**, 7005 (1997); Q. Chen, S. Chen, and G. L. Eyink, Phys. Fluids **15**, 361 (2003); Q. Chen, S. Chen, G. L. Eyink, and D. D. Holm, Phys. Rev. Lett. **90**, 214503 (2003); D. O. Gómez and P. D. Mininni, Physica A **342**, 69 (2004); P. D. Mininni, A. Alexakis, and A. Pouquet, Phys. Rev. E **74**, 016303 (2006).
- [9] A. Brissaud, U. Frisch, J. Leorat, M. Lesieur, and A. Mazure, Phys. Fluids. **16**, 1366 (1973).
- [10] G. Krstulovic, P. D. Mininni, M. E. Brachet, and A. Pouquet, Phys. Rev. E **79**, 056304 (2009).
- [11] R. J. Donnelly, “it Quantized Vortices in Helium II” (Cambridge University Press, Cambridge, 1991).
- [12] M. Tsubota, K. Kasamatsu, and M. Kobayashi in “*Novel Superfluid: Quantized vortices in superfluid helium and atomic Bose-Einstein condensates*”, International Series of Monographs on Physics, edited by K. H. Bennemann and J. B. Ketterson (Oxford Science Publications, Oxford, 2013).
- [13] P. Clark di Leoni, P. D. Mininni, and M. E. Brachet, Phys. Rev. A **94**, 043605 (2016); P. Clark di Leoni, P. D. Mininni, and M. E. Brachet, arXiv:1705.03525.
- [14] The topological charges of quantized vortices are defined by the fundamental group π_1 of the order-parameter manifold G/H of the system, where G is the symmetry of the Hamiltonian and H is the remaining symmetry of the order parameter. In general, three distinct definitions can be adopted for non-Abelian (Abelian) vortices: (i) G is non-Abelian (Abelian), (ii) H is non-Abelian (Abelian), and (iii) $\pi_1(G/H)$ is non-Abelian (Abelian). We adopt definition (iii) in this Letter because it is directly connected to the collision dynamics of quantized vortices.
- [15] J. Koplik and H. Levine, Phys. Rev. Lett. **71**, 1375 (1993); **76**, 4745 (1996); M. Leadbeater, T. Winiecki, D. C. Samuels, C. F. Barenghi, and C. S. Adams, Phys. Rev. Lett. **86**, 1410 (2001).
- [16] M. Kobayashi, Y. Kawaguchi, M. Nitta, and M. Ueda, Phys. Rev. Lett. **103**, 115301 (2009).
- [17] Y. Kawaguchi and M. Ueda, Phys. Rep. **520** 253 (2010).
- [18] H. Mäkelä, Y. Zhang, and K-A Suominen, J. Phys. A **36**, 8555 (2003); H. Mäkelä, J. Phys. A **39**, 7423 (2006); F. Zhou and G. W. Semenoff, Phys. Rev. Lett. **97**, 180411 (2006).
- [19] M. Koashi and M. Ueda, Phys. Rev. Lett. **84**, 1066 (2000); M. Ueda and M. Koashi, Phys. Rev. A **65**, 063602 (2002); H. Saito and M. Ueda, Phys. Rev. A **72**, 053628 (2005).
- [20] In the cyclic phase, ψ_{cyclic} is invariant under the following 12 transformations [18]: $\mathbf{1}$, $I_{x,y,z} = e^{-i\hat{S}_{x,y,z}\pi}$, $C = e^{2\pi i/3} e^{-2\pi i(\hat{S}_x + \hat{S}_y + \hat{S}_z)/(3\sqrt{3})}$, C^2 , $I_{x,y,z}C$, and $I_{x,y,z}C^2$. These 12 transformations form the non-Abelian tetrahedral group. Topological charges of vortices can be classified by 12 elements $\mathbf{1}$, $I_{x,y,z}$, \dots of the non-Abelian tetrahedral group. Details are reviewed in M. Kobayashi, J. Phys. Conf. Ser. **297**, 021013 (2011) for order parameters and circulations of each vortices, and S. Kobayashi, *et. al.*, Nucl. Phys. B **856**, 577 (2012) for the classification of topological charges by the fundamental group.
- [21] C. Nore, M. Abid, and M. E. Brachet, Phys. Rev. Lett. **78**, 3896 (1997).
- [22] For the details about how to numerically obtain the vortex length density ρ_{vortex} , see M. Kobayashi and L. F. Cugliandolo, Phys. Rev. E **94**, 062146 (2016).
- [23] M. Kobayashi and M. Tsubota, Phys. Rev. Lett. **94**, 065302 (2005); J. Phys. Soc. Jpn. **74**, 3248 (2005).
- [24] A. Villois, D. Proment, and G. Krstulovic, Phys. Rev. E **93**, 061103(R) (2016).
- [25] M. W. Scheeler, D. Kleckner, D. Proment, G. L. Kindlmann, and W. T. M. Irvine, Proc. Natl. Acad. Sci. USA **111**, 15350 (2014).
- [26] C. F. Barenghi, Milan J. Math. **75**, 177 (2007).
- [27] L. Biferale, S. Musacchio, and F. Toschi, Phys. Rev. Lett. **108**, 164501 (2012).
- [28] P. M. Chaikin and T. C. Lubensky, “*Principles of Condensed Matter Physics*” (Cambridge University Press, Cambridge 2000).
- [29] V. Parnaru and G. Toulouse, J. Phys. (Paris) **38** 887, (1977); N. D. Mermin, Rev. Mod. Phys. **51**, 591 (1979).
- [30] A. Vilenkin and E. P. S. Shellard, “*Cosmic Strings and Other Topological Defects*” (Cambridge University Press, Cambridge, 1994); M. B. Hindmarsh and T. W. B. Kibble, Rep. Prog. Phys. **58**, 477 (1995).
- [31] D. N. Spergel and U. L. Pen, Astrophys. J. **491**, L67 (1997); P. McGraw, Phys. Rev. D **57**, 3317 (1998); M. Bucher and D. N. Spergel, Phys. Rev. D **60**, 043505 (1999).
- [32] R. Tamagaki, Prog. Theor. Phys. **44**, 905 (1970).